Optics Communications 437 (2019) 90–94

Contents lists available at ScienceDirect

Optics Communications

journal homepage: www.elsevier.com/locate/optcom

Curved volume waveguides induced by Airy beams in negative polarizability nanosuspensions

Xinli Liang [a], Ze Zhang [a,*], Deng Li [a], Xiaofang Han [b], Feng Gao [b], Zhigang Chen [b]

[a] Aerospace Information Research Institute, Chinese Academy of Sciences, Beijing, 100094, China
[b] MOE Key Laboratory of Weak-Light Nonlinear Photonics, TEDA Institute of Applied Physics and School of Physics, Nankai University, Tianjin 300457, China

ARTICLE INFO

Keywords:
Nonlinear soft-matter
Curved nonlinear guided waves
Optical solitons
Airy beams

ABSTRACT

In this paper, we theoretically analyze the formation of stable curved volume waveguides with nonlinear optical induction by Airy beams in colloidal nanosuspensions with negative polarizability. Numerical simulations are performed to show how to modify the waveguide structures by actively control of the conditions for Airy beam generation, including the truncation factor, transverse scale, and launching direction. Possible applications of such curved waveguides are discussed.

1. Introduction

Ever since Ashkin and his coworkers demonstrated that micro-particles can be manipulated with laser beam, the study of the interaction between light and micro-particles has always been a hot topic in several areas [1–3]. One of these areas is the optical soft matter of colloidal nanosuspensions, in which nano-particles are suspended in liquid background media. When a laser beam is incident into the nanosuspension media, nano-particles can be pulled in or pushed out of the laser beam due to the gradient force, thus causing different nonlinear effects [4–6]. Typically, there are two kinds of nonlinearities: one is Kerr-like non-saturable nonlinearity which generally happens in a positive-polarizability nanosuspension (PPN), in which the refractive index of particles n_p is higher than that of the background liquid n_b(i.e., $n_p > n_b$); the other is saturable nonlinearity which generally happens in a negative-polarizability nanosuspension (NPN), in which the refractive index of particles n_p is lower than n_b(i.e., $n_p < n_b$) [4,7,8]. PPN has always been a "good candidate" for generating solitons or waveguide structures since it is very easy to be prepared [9–13]. Recently, it has been shown that the NPN exhibits saturable nonlinear response which can be used to form stable solitons or other kinds of self-guided optical structures [14–16], and thus attracted a lot of attention [17,18]. However, thus far, there is still no report on light-induced curved waveguides yet, which are essentially important in applications such as 3D-integrated-photonics and laser beam combination. Here, we propose theoretically a method to generate curved waveguides in NPN with self-accelerating Airy beams, along with numerical simulations of the dynamics process.

The outline of the paper is as follows: In Section 2, we theoretically demonstrate the mechanism to induce curved waveguides, and analyze their typical properties; In Section 3, to verify the theoretical predications, we numerically simulate the process to induce curved waveguides in the NPN made by polytetrafluoroethylene (PTFE) (n = 1.34) and glycerin (n = 1.47), and observe the characteristic changes by controlling the propagation behavior of Airy beams; In Section 4, we summarize our results and discuss possible experimental realization and future applications.

2. Theoretical analysis

In dielectric nanosuspensions, the nonlinearity is mainly from the optical forces exerted by a light beam with a spatially varying intensity, which causes a redistribution of particles in the medium, generating, in turn, an effective refractive index change which modifies light propagation. In low concentration condition, the many-body effect can be ignored, so the effective refractive index [4,19] in the nanosuspension can be simplified as:

$$n_{\mathrm{eff}}(x, y) = n_b + (n_p - n_b)V_p\rho_0 \exp\left(\frac{\alpha I}{4k_B T}\right), \tag{1}$$

where n_b is the refractive index of the background medium, n_p is refractive index of the particle and $m = n_p/n_b$ is the ratio of the particle refractive index to the background medium refractive index. V_p is volume of an individual particle, ρ_0 stands for the unperturbed uniform particle density, $\alpha = 3V_p\varepsilon_0 n_b^2\left(\frac{m^2-1}{m^2+2}\right)$ is the polarizability, ε_0 is the permittivity of vacuum, I is the intensity of induced beam, k_B represents the Boltzmann constant, and T represents temperature.

When a finite energy Airy beam is used as the waveguide-inducing light field, the intensity of Airy beam can be given as

$$I = U_{\mathrm{Ai}}U_{\mathrm{Ai}}^*, \tag{2}$$

* Corresponding author.
E-mail address: zhangze@aoe.ac.cn (Z. Zhang).

https://doi.org/10.1016/j.optcom.2018.12.054
Received 3 September 2018; Received in revised form 10 December 2018; Accepted 14 December 2018
Available online 18 December 2018
0030-4018/

where

$$U_{\mathrm{Ai}} = A_0\mathrm{Ai}(x/x_0)\mathrm{Ai}(y/x_0)\exp(a\ x/x_0) \times\exp(a\ y/x_0)\exp(iv\ x/x_0)\exp(iv\ y/x_0), \tag{3}$$

Ai represents the Airy function, A_0 is the amplitude, x_0 is arbitrary transverse scale, v is normalized initial launch angle, and a is the truncation factor.

In an NPN, where particles have lower refractive index than background medium (i.e., $\alpha < 0$), the effective refractive index is proportional to light intensity exponentially. In this case, particles are repelled from the beam center by optical gradient force. When light intensity gradually increases, it is possible to form a distribution with high refractive index at the beam center and low refractive index at the edge, which is similar as a 'waveguide'. If light intensity increases to a certain value, the difference between refractive index at the beam center and edge could get to its maximum. At this time, the nonlinearity of nanosuspension reaches its saturable state, so the generated waveguides could be stable even at high laser power. Moreover, Airy beams accelerate transversely during propagation [20], which means its propagation path is curved. From Eq. (1) we can see that the effective refractive index distribution changes with light intensity exponentially, which means curved volume waveguide structures can be induced by Airy beams in NPN. The characteristics of the curved waveguide induced by Airy beams are analyzed below in detail.

2.1. Size

To define the size of a waveguide, we need to find the refractive index jump which is usually at the interface between the core and cladding. For convenience, here we consider one-dimensional (1D) case. The calculation of two-dimensional case can be easily extended from one-dimensional case.

To observe the change of $n_{\mathrm{eff}}(x)$, we take the first-order derivative of Eq. (1) and get,

$$n'_{\mathrm{eff}} = (n_{\mathrm{p}} - n_{\mathrm{b}})V_{\mathrm{p}}\rho_0\exp(\frac{\alpha I}{4k_BT})\frac{\alpha A_0^2}{2x_0k_BT}\exp(2a\frac{x}{x_0}) \times\mathrm{Ai}(\frac{x}{x_0})\left[\mathrm{Ai}'(\frac{x}{x_0}) + a\mathrm{Ai}(\frac{x}{x_0})\right]. \tag{4}$$

With $n'_{\mathrm{eff}} = 0$, we can get two positions (x_1, x_2) around the main lobe where the refractive index changes most slowly. In which, we use the parameters as those from previous experiments [14]: the PTFE particles ($n_{\mathrm{p}} = 1.34$) of radius 50 nm are suspended in glycerin ($n_{\mathrm{b}} = 1.47$) and water mixture at a concentration of $1.9 \times 10^{11}/\mathrm{cm}^3$ (volume filling factor $f_{\mathrm{p}} = 10^{-4}$)

$$x_1 = -2.338x_0, \tag{5}$$

$$x_2 = (2.394 + 5.988a - 8.770a^2 + 5.653a^3)x_0. \tag{6}$$

According to the definition of waveguides, $|x_1x_2|$ can be defined as the total size of generated waveguide. Then, we take the second-order derivative of Eq. (1), and get,

$$\begin{aligned} n''_{\mathrm{eff}} = {} & (n_{\mathrm{p}} - n_{\mathrm{b}})V_{\mathrm{p}}\rho_0\exp(\frac{\alpha I}{4k_BT})\frac{\alpha A_0^2}{2x_0{}^2k_BT}\exp(2a\frac{x}{x_0}) \\ & \times[\frac{\alpha A_0^2}{2k_BT}\exp(2a\frac{x}{x_0})\mathrm{Ai}^2(\frac{x}{x_0})(\mathrm{Ai}'(\frac{x}{x_0}) + a\mathrm{Ai}(\frac{x}{x_0}))^2 \\ & + (\mathrm{Ai}'(\frac{x}{x_0}) + a\mathrm{Ai}(\frac{x}{x_0}))(\mathrm{Ai}'(\frac{x}{x_0}) + 2a\mathrm{Ai}(\frac{x}{x_0})) \\ & + \mathrm{Ai}(\frac{x}{x_0})(\mathrm{Ai}''(\frac{x}{x_0}) + a\mathrm{Ai}'(\frac{x}{x_0}))]. \end{aligned} \tag{7}$$

With $n''_{eff} = 0$, we get another two positions (x_3, x_4) around the main lobe where the refractive index changes most quickly:

$$\begin{aligned} x_3 = {} & \{(0.384 + 0.244a + 0.540a^2 - 0.227a^3) \\ & \times\exp[\frac{\alpha A_0^2}{2k_BT(13.869 + 15.769a + 68.123a^2 - 62.206a^3)}] \\ & - 2.339 + 0.205exp(1.446a)\} \times x_0, \end{aligned} \tag{8}$$

$$\begin{aligned} x_4 = {} & \{[1.413exp(\alpha A_0^2/13.176k_BT) + 0.506] \\ & \times exp[\frac{a}{0.777exp(\alpha A_0^2/14.267k_BT) - 0.644}] \\ & - 2.347exp(\alpha A_0^2/20.137k_BT) + 0.129\} \times x_0. \end{aligned} \tag{9}$$

$|x_3x_4|$ can be defined as the core size of the waveguide. The rest parts $|x_1x_3|$ and $|x_2x_4|$ can be defined as the cladding size of the waveguide. According to Eqs. (5), (6), (8), (9), the waveguide size is affected by truncation factor, polarizability and light intensity, as shown in Fig. 1. The blue curves represent the total size of the waveguide, and the red curves represent the core size. Fig. 1(a) shows the relation between the waveguide size and the truncation factor, from which we can see that the total waveguide size increases nearly linearly with the truncation factor, whereas the core size is nearly inversely proportional to the truncation factor. In fact, the truncation factor a determines the proportion of energy carried by the main lobe of the Airy beam: a larger a corresponds to more energy carried by the main lobe. In the induced waveguide structure, the energy of the main lobe plays a major role, while the energy of the sidelobes has an adverse effect. By controlling the truncation factor, the size of the induced waveguide can be controlled. Fig. 1(b) shows the relation between waveguide size and polarizability. The calculation shows that the total size does not change with the polarizability. As for the core size, when the polarizability is smaller than -0.5×10^{-20} F m^2, it does not change with polarizability; when the polarizability is larger than -0.5×10^{-20} F m^2, the core size decreases with the increase of polarizability. Fig. 1(c) shows that the total waveguide size does not change with light intensity, while the core size increases rapidly as the light intensity increase. In conclusion, the total size of the waveguide could be optimized by controlling the truncation factor, while the core size of the waveguide could be modified by changing the truncation factor, polarizability, as well as light intensity. Besides that, the size of the waveguide is also related to the size of Airy beams' main lobe, which is usually determined by the optical aperture and focal length in reality.

Similarly with a conventionally fabricated waveguide, the numerical aperture of the induced curved waveguide can be defined as:

$$NA(x) = \sqrt{n_{\mathrm{eff}}{}^2(x) - n^2} \qquad x \in [x_3, x_4], \tag{10}$$

where $n = n_{\mathrm{b}} + (n_{\mathrm{p}} - n_{\mathrm{b}})f$ is the refractive index of cladding layer.

2.2. Curvature

If the path of a generated 1D waveguide is written as $x(z)$, then the first derivative $\frac{\mathrm{d}x}{\mathrm{d}z}$ determines the slope of $x(z)$, while the second derivative $\frac{\mathrm{d}^2x}{\mathrm{d}z^2}$ determines the change rate of slope, which means the convexity ratio of $x(z)$ when $\frac{\mathrm{d}^2x}{\mathrm{d}z^2} > 0$, or the concavity ratio of $x(z)$ when $\frac{\mathrm{d}^2x}{\mathrm{d}z^2} < 0$. For most of applications, only the absolute value of $\frac{\mathrm{d}^2x}{\mathrm{d}z^2}$ is concerned, so we use $\left|\frac{\mathrm{d}^2x}{\mathrm{d}z^2}\right|$ to determine the curvature of generated waveguides in this paper.

As demonstrated in reference [21], Airy beams travel along parabolic trajectory in Kerr medium. The light field of a finite energy Airy beam can be written as [22]:

$$\begin{aligned} \varphi(s,\xi) = {} & A_0\mathrm{Ai}(s - (\frac{\xi}{2})^2 - v\xi + ia\xi) \times\exp(as - \frac{a\xi^2}{2} \\ & - av\xi - i\frac{\xi^3}{12} + i\frac{a^2\xi}{2} - i\frac{v^2\xi}{2} + i\frac{s\xi}{2} + ivs - i\frac{v\xi^2}{2}), \end{aligned} \tag{11}$$

where $s = x/x_0$ represents a dimensionless transverse coordinate, $\xi = z/kx_0^2$ represents normalized propagation distance. When $a = 0$, Eq. (11) equals to one which describes infinite energy Airy beams [23].

For an infinite energy Airy beam, the beam follows a ballistic trajectory in the s–ξ plane that is described by the parabola $s = (\frac{\xi}{2})^2 + v\xi$. In $x - z$ coordinate, it can be written as:

$$x = \frac{\lambda^2}{(16\pi^2x_0^3)}(z + \frac{8\pi^2x_0^3\theta}{\lambda^2})^2 - \frac{4\pi^2x_0^3\theta^2}{\lambda^2}, \tag{12}$$

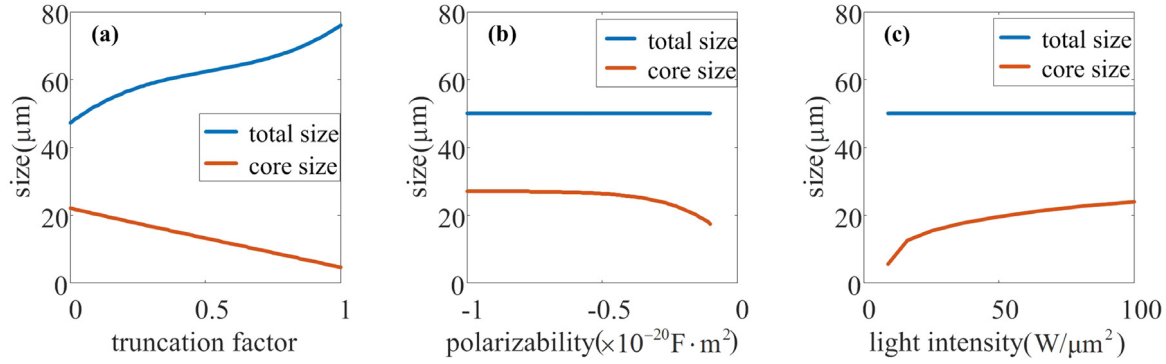

Fig. 1. The change of waveguide size as a function of (a) truncation factor, (b) polarizability, and (c) light intensity.

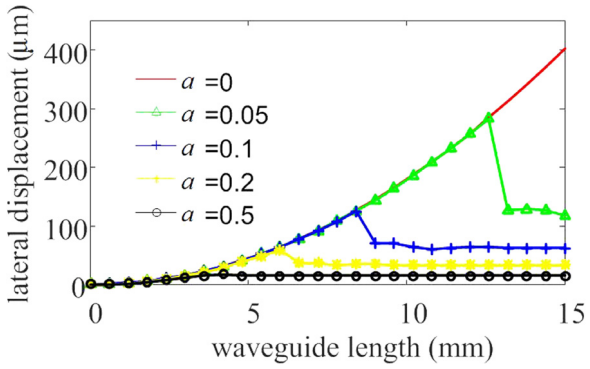

Fig. 2. The curved waveguide path induced with Airy beams of different truncation factors.

where $\theta = v/(kx_0)$ is the actual launch angle in $x-z$ coordinate.

The second derivative of Eq. (12) is:

$$\frac{\mathrm{d}^2x}{\mathrm{d}z^2} = \frac{\lambda^2}{8\pi^2 x_0^3}. \tag{13}$$

From Eq. (13) we can see that the curvature of induced waveguide is affected by two factors: transverse scale and wavelength. In reality, the physical picture of the transverse scale should be optical aperture and focal length, or beam size in essence. By changing the size and wavelength of Airy beams during the generation procedure of waveguides, waveguides in different curvature can be generated.

However, the propagation of finite energy Airy beams is somewhat different with that of infinite energy ones since their tails are truncated by apertures. To study the curvature of waveguide induced by finite Airy beams, we define the waveguide center as the point with maximum refractive index. In this case, we can calculate the position of waveguide center at different lengths, and depict the curved structure with these position points, as shown in Fig. 2. It illustrates that waveguides generated by Airy beams with different truncation factors have the similar curvature at the beginning, but deviate from each other in later process. The bigger the truncation factor is, the further the waveguides deviate from the ideal path.

2.3. Direction and length

Inspired by the work in Refs. [24,25], it is possible to change the actual initial launch angle of Airy beams to generate curved waveguides with different directions. The parabolic trajectory can be shifted upward, when an Airy beam is launched downwards ($\theta < 0$). In this case, the generated waveguides are up-skew. In the same way, the down-skew waveguides could be stimulated by the downward parabolic trajectory, when the Airy beam is launched upwards ($\theta > 0$). Otherwise, if an Airy beam is launched horizontally, the generated waveguides are horizontal in the beginning and down-skew in the rear.

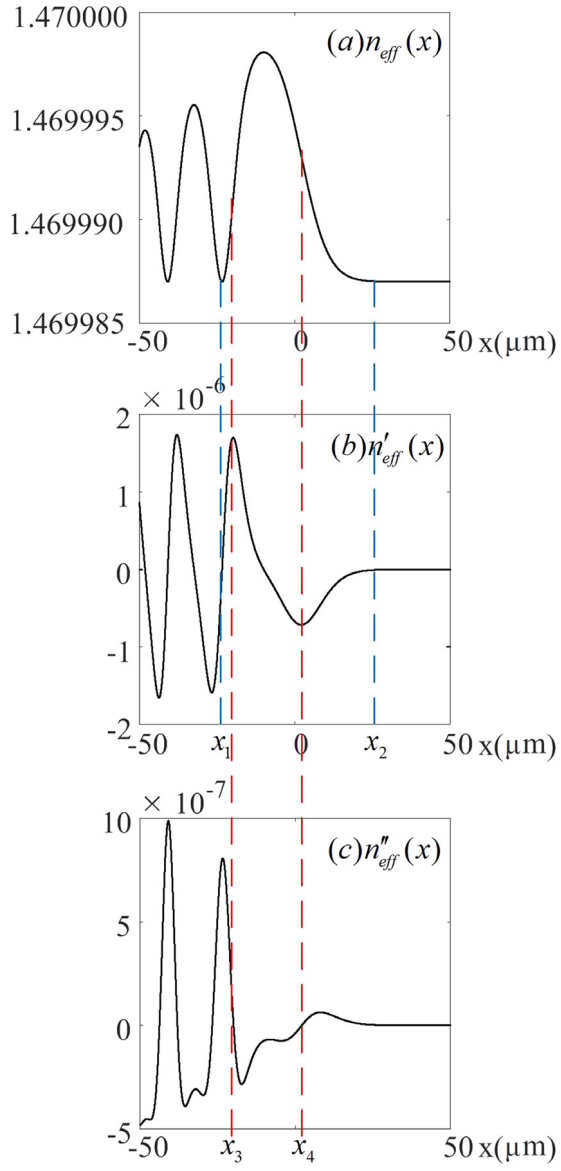

Fig. 3. Calculated effective refractive index distribution (a) and its first order (b) and second order (c) derivatives. The vertical dashed lines are added as reference for waveguide size.

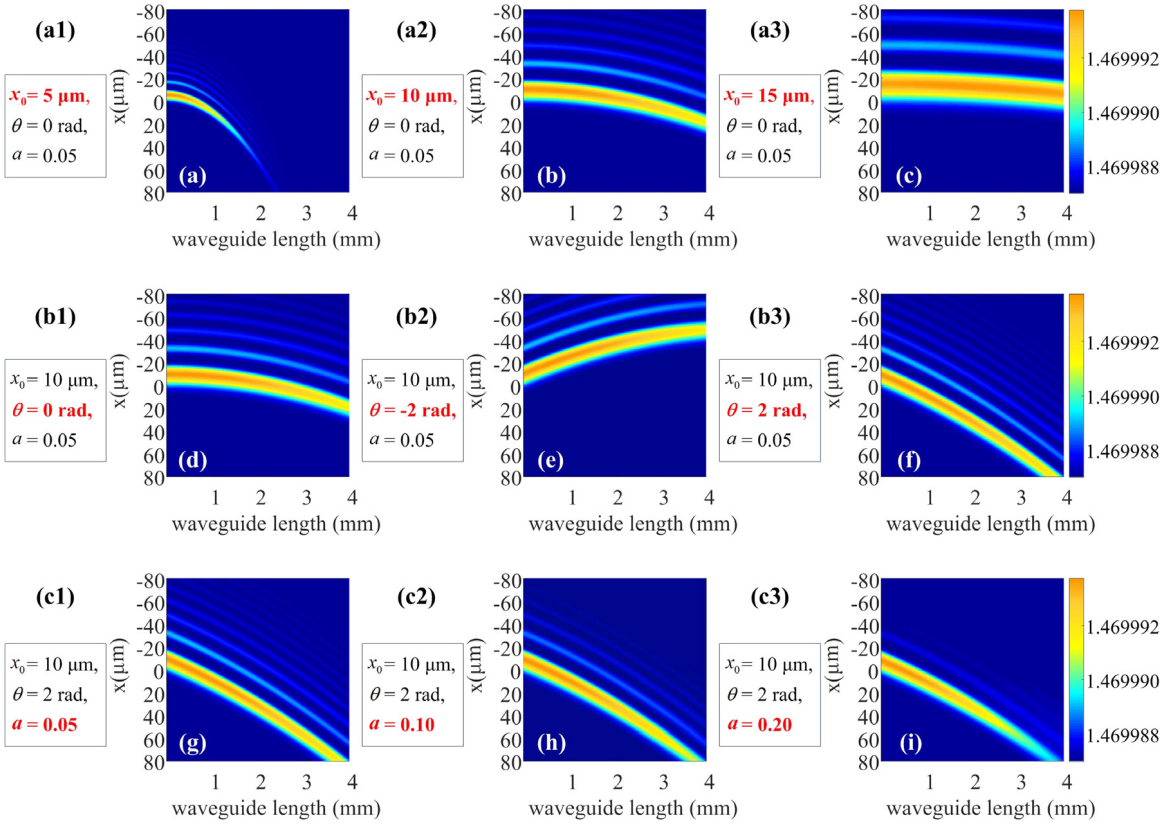

Fig. 4. Curved waveguide structure induced by Airy beams with different parameters: (a1) $x_0 = 5$ μm, $\theta = 0$ rad, $a = 0.05$. (a2) $x_0 = 10$ μm, $\theta = 0$ rad, $a = 0.05$. (a3) $x_0 = 15$ μm, $\theta = 0$ rad, $a = 0.05$. (b1) $x_0 = 10$ μm, $\theta = 0$ rad, $a = 0.05$. (b2) $x_0 = 10$ μm, $\theta = -2$ rad, $a = 0.05$ (b3) $x_0 = 10$ μm, $\theta = 2$ rad, $a = 0.05$. (c1) $x_0 = 10$ μm, $\theta = 2$ rad, $a = 0.05$. (c2) $x_0 = 10$ μm, $\theta = 2$ rad, $a = 0.10$. (c3) $x_0 = 10$ μm, $\theta = 2$ rad, $a = 0.20$.

In addition, the length and energy of the main lobe of Airy beams mainly depends on the truncation factor a. The bigger the truncation factor is, the less energy the main lobe carries and the shorter the main lobe propagates. In this way, the length of curved waveguides could be controlled by changing factor a.

3. Numerical simulation

As discussed above, particles in NPN are repelled away from the beam center when Airy beams are incident into nanosuspension, and thus a waveguide structure with higher refractive index in the center could be built. As laser power increases, more and more particles are repelled, so the self-induced transparency effect starts to appear. Therefore, longer and clearer waveguide structure could be generated.

In this part, we observe the generation procedure of waveguides induced by Airy beams with different power in simulation. To be close to the actual situation, we use the parameters of a common NPN, in which PTFE particles ($n_p = 1.34$) of radius 50 nm are suspended in glycerin ($n_b = 1.47$) at a concentration of 1.9×10^{11} / cm^3 (volume filling factor $f_p = 10^{-4}$). Airy beams with parameters of $\lambda = 532$ nm, $x_0 = 10$ μm, $\theta = 0°$, $a = 0.05$ are used as the induced beam.

In the simulation, waveguide length is defined as the length from beginning to the position where the value of center refractive index reduces to that of cladding. The simulation results show that waveguides with length of 2.7 mm, 4.7 mm and 5.6 mm can be generated when light intensity is set as 25 W/μm^2, 64 W/μm^2 and 100 W/μm^2, respectively. As predicted above, simulation shows that the waveguide structure does not break at all even at very high power because of the saturable nature of the nonlinearity in NPN.

With specific parameters of $x_0 = 10$ μm, $a = 0.05$, we simulate the generation of waveguide structure when light intensity is set as 64 W/μm^2. The typical transverse coordinates of waveguide is measured as $x_1 = -23.38$ μm, $x_2 = 26.72$ μm, $x_3 = -19.63$ μm, $x_4 = 1.54$ μm. Thus, the size of the whole waveguide and the size of its core are calculated to be 50.10 μm and 21.17 μm, respectively. The corresponding curves of n_{eff}, n'_{eff}, n''_{eff} and waveguide sizes are shown in Fig. 3.

Besides the size and length, the curvatures of generated waveguides can also be adjusted by changing the transverse scale of Airy beams. In simulation, we observe that the curvature, length and lateral displacement of generated waveguide are approximate 2.87×10^{-5} μm^{-1}, 1.2 mm and 20.65 μm, respectively, when the transverse scale is set as 5 μm, as shown in Fig. 4 (a1). The curvature and lateral displacement changes to 3.59×10^{-6} μm^{-1} and 28.68 μm at the propagation distance of 4 mm when the transverse scale is 10 μm, as shown in Fig. 4 (a2). When the transverse scale is increased to 15 μm, the curvature and lateral displacement are about 1.06×10^{-6} μm^{-1} and 8.50 μm at the propagation distance of 4 mm, as shown in Fig. 4 (a3). Thus, we can conclude that the bigger the transverse scale is, the smaller the curvature is. Meantime, we can also see that with a bigger transverse scale, the induced waveguide size is also bigger.

To see the direction and length of induced waveguides affected by launch angle and truncation factors, we still set the parameters of NPN as we used above while launch angle and the truncation factors of incident beam are set as $\theta = 0$ rad, $\theta = -2$ rad, $\theta = 2$ rad, and $a = 0.05$, $a = 0.1$, $a = 0.2$, respectively. The simulation results are shown in Fig. 4. We can see that waveguides with different directions can be generated if Airy beams with different launch angles are incident into NPN, as shown in Fig. 4 (b1, b2, b3). Besides the transverse scale, the truncation factors can also affect the length of generated waveguide. As shown in Fig. 4 (c1, c2, c3), with bigger truncation factor, shorter waveguide would be generated. It means the length of induced waveguides can also be controlled by changing transverse scale and truncation factor of Airy beams.

4. Summary

As a conclusion, we have presented our theoretical analysis and numerical simulation of curved waveguides optically induced in NPN (an experimentally feasible soft-matter system, as demonstrated previously). As shown in our study, by controlling incident Airy beams' propagation behavior, curved waveguide structure with different size, curvature, length and direction can be generated in NPN. The simulation results have good agreement with theoretical predication. Our results indicate that curved waveguide structures are possible and can be induced in a bulk medium, which is promising for many applications such as in beam coherent combining, optical manipulation and 3D-integrated-photonics. Based on our study, the curved waveguides could be predesigned which is not only useful for the further experimental implementation but also important in practical applications of engineered photonic devices based on the solidifying the NPN by cooling, ultraviolet radiation or other methods.

Acknowledgments

This work is financially supported by the Natural National Science Foundation of China (Grant NOs. 61475161 and 11574161) and the National Key R&D Program of China (Grant No. 2017YFA0303800).

References

[1] A. Ashkin, J.M. Dziedzic, P.W. Smith, Continuous-wave self-focusing and self-trapping of light in artificial Kerr media, Opt. Lett. 7 (1982) 276–278, http://dx.doi.org/10.1364/OL.7.000276.

[2] A. Ashkin, J.M. Dziedzic, J.E. Bjorkholm, S. Chu, Observation of a single-beam gradient force optical trap for dielectric particles, Opt. Lett. 11 (1986) 288–290, http://dx.doi.org/10.1364/OL.11.000288.

[3] A. Ashkin, J.M. Dziedzic, Optical trapping and manipulation of viruses and bacteria, Science 235 (1987) 1517–1520, http://dx.doi.org/10.1126/science.3547653.

[4] R. El-Ganainy, D.N. Christodoulides, C. Rotschild, M. Segev, Soliton dynamics and self-induced transparency in nonlinear nanosuspensions, Opt. Express 15 (2007) 10207–10218, http://dx.doi.org/10.1364/OE.15.010207.

[5] M. Matuszewski, W. Krolikowski, Y.S. Kivshar, Spatial solitons and light-induced instabilities in colloidal media, Opt. Express 16 (2008) 1371–1376, http://dx.doi.org/10.1364/OE.16.001371.

[6] M. Matuszewski, W. Krolikowski, Y.S. Kivshar, Soliton interactions and transformations in colloidal media, Phys. Rev. A 79 (2009) 023814, http://dx.doi.org/10.1103/PhysRevA.79.023814.

[7] Z. Chen, M. Segev, D.N. Christodoulides, Optical spatial solitons: historical overview and recent advances, Rep. Progr. Phys. 75 (2012) 086401, http://dx.doi.org/10.1088/0034-4885/75/8/086401.

[8] S. Biria, D.R. Morim, F.A. Tsao, K. Saravanamuttu, I.D. Hosein, Coupling nonlinear optical waves to photoreactive and phase-separating soft matter: Current status and perspectives, Chaos 27 (2017) 104611, http://dx.doi.org/10.1063/1.5001821.

[9] Y.S. Kivshar, G.I. Stegeman, Spatial optical solitons, Opt. Photonics News 13 (2002) 59–63, http://dx.doi.org/10.1364/OPN.13.2.000059.

[10] W.M. Lee, R. El-Ganainy, D.N. Christodoulides, K. Dholakia, E.M. Wright, Nonlinear optical response of colloidal suspensions, Opt. Express 17 (2009) 10277–10289, http://dx.doi.org/10.1364/OE.17.010277.

[11] R.A. Terborg, J.P. Torres, K. Volke-Sepulveda, Steering and guiding light with light in a nanosuspension, Opt. Lett. 38 (2013) 5284–5287, http://dx.doi.org/10.1364/OL.38.005284.

[12] L.A. López-Peña, Y. Salazar-Romero, R.A. Terborg, J. Hernández-Cordero, J.P. Torres, K. Volke-Sepúlveda, Waveguides in colloidal nanosuspensions, Proc. SPIE 9164 (2014) 916429, http://dx.doi.org/10.1117/12.2064341.

[13] M.Y. Salazar-Romero, Y.A. Ayala, E. Brambila, L.A. Lopez-Peña, L. Sciberras, A.A. Minzoni, R.A. Terborg, J.P. Torres, K. Volke-Sepúlveda, Steering and switching of soliton-like beams via interaction in a nanocolloid with positive polarizability, Opt. Lett. 42 (2017) 2487–2490, http://dx.doi.org/10.1364/OL.42.002487.

[14] W. Man, S. Fardad, Z. Zhang, J. Prakash, M. Lau, P. Zhang, M. Heinrich, D.N. Christodoulides, Z. Chen, Optical nonlinearities and enhanced light transmission in soft-matter systems with tunable polarizabilities, Phys. Rev. Lett. 111 (2013) 218302, http://dx.doi.org/10.1103/PhysRevLett.111.218302.

[15] S. Fardad, Particle Manipulation via Optical Forces and Engineering Soft-Matter Systems with Tunable Nonlinearities (Doctoral Dissertation), University of Central Florida, 2014.

[16] S.Z. Silahli, W. Walasik, N.M. Litchinitser, Necklace beam generation in nonlinear colloidal engineered media, Opt. Lett. 40 (2015) 5714–5717, http://dx.doi.org/10.1364/OL.40.005714.

[17] S. Fardad, M.S. Mills, P. Zhang, W. Man, Z. Chen, D.N. Christodoulides, Interactions between self-channeled optical beams in soft-matter systems with artificial nonlinearities, Opt. Lett. 38 (2013) 3585–3587, http://dx.doi.org/10.1364/OL.38.003585.

[18] J. Sun, S.Z. Silahli, W. Walasik, Q. Li, E. Johnson, N.M. Litchinitser, Nanoscale orbital angular momentum beam instabilities in engineered nonlinear colloidal media, Opt. Express 26 (2018) 5118–5125, http://dx.doi.org/10.1364/OE.26.005118.

[19] J.C.M. Garnett, XII. Colours in metal glasses and in metallic films, Philos. Trans. R. Soc. Lond. A Math. Phys. Eng. Sci. 203 (1904) 385–420, http://dx.doi.org/10.1098/rsta.1904.0024.

[20] G.A. Siviloglou, J. Broky, A. Dogariu, D.N. Christodoulides, Observation of accelerating Airy beams, Phys. Rev. Lett. 99 (2007) 213901, http://dx.doi.org/10.1103/PhysRevLett.99.213901.

[21] R. Chen, C. Yin, X. Chu, H. Wang, Effect of Kerr nonlinearity on an Airy beam, Phys. Rev. A 82 (2010) 043832, http://dx.doi.org/10.1103/PhysRevA.82.043832.

[22] G.A. Siviloglou, J. Broky, A. Dogariu, D.N. Christodoulides, Ballistic dynamics of Airy beams, Opt. Lett. 33 (2008) 207–209, http://dx.doi.org/10.1364/OL.33.000207.

[23] G.A. Siviloglou, D.N. Christodoulides, Accelerating finite energy Airy beams, Opt. Lett. 32 (2007) 979–981, http://dx.doi.org/10.1364/OL.32.000979.

[24] Y. Hu, P. Zhang, C. Lou, S. Huang, J. Xu, Z. Chen, Optimal control of the ballistic motion of Airy beams, Opt. Lett. 35 (2010) 2260–2262, http://dx.doi.org/10.1364/OL.35.002260.

[25] Y. Hu, G.A. Siviloglou, P. Zhang, N.K. Efremidis, D.N. Christodoulides, Z. Chen, Self-accelerating Airy beams: generation, control, and applications, in: Nonlinear Photonics and Novel Optical Phenomena, Springer, New York, 2012, pp. 1–46.